Provision of Ancillary Services utilizing a Network of Fast-Charging Stations for Electrical Buses

Ioannis Lymperopoulos[1], Faran A. Qureshi[2], Altug Bitlislioglu[2], Jan Poland[1], Alessandro Zanarini[1], Mehmet Mercangoez[1], and Colin Jones[2]

[1]ABB Corporate Research Center, Switzerland
[2]Automatic Control Laboratory, EPFL, Switzerland

October 18, 2018

Abstract

We demonstrate how charging infrastructure for electrical vehicles can be utilized for the provision of Ancillary Services to the Power Grid. Fast-charging stations that supply energy to vehicles at high power rates incorporate energy storage to prevent high currents to the grid and to avoid peak-demand price charges. A network of charging stations with storage has also the potential to generate Ancillary Services. The main challenge is in the synchronization between the stochastic demand for control energy and the requirements for fast-charging services from arriving electrical vehicles. The method presented first calculates the maximum capacity of control-energy the system can provide and during operation delivers it to the grid upon request, while it continuously provides fast-charging services to the vehicles. To showcase our concept we utilize the ABB TOSA electrical bus charging network and the Ancillary Services requirements of Swissgrid, the Transmission System Operator of Switzerland. We show, through our simulation studies, using realistic models and energy prices, that the method is technically feasible, can deliver a considerable level of control energy and has a minor impact on the lifetime of the storage system, while generating substantial economic advantages.

ancillary services, electric vehicles, secondary frequency control, fast-charging, energy storage, smart grids, stochastic optimization, MPC.

1 Introduction

Electrification in transportation is projected to grow intensively in the upcoming decades, reaching 100s of millions of electric vehicles on the roads [1,2]. Adoption of electrical vehicles is expected to have an impact both on energy generation, but also on power distribution. Networks of charging stations, either commercial or residential, will impact the power-grid by imposing on it the consumption profile of vehicles. The requirement for fast-charging will also have an impact on the real-time stability of the power grid and for this reason many fast-charging

Figure 1: The bus recharges at stops using its roof-mounted contacts that engage automatically using laser guidance. It takes less than 1 sec to connect the bus to the charging contact.

stations will incorporate energy storage that acts as a buffer between the vehicles and the grid. This uncertainty and variability will be added to the effects of the mass integration of Renewable Energy Sources (RES) to the power grid, that have been extensively discussed and analyzed [3].

The generation of Ancillary Services (AS) by utilizing novel assets, such as loads, storage systems, or distributed generation, is expected to mitigate those effects and allow for high penetration of RES and electric vehicles [4]. Storage systems are expected to play a substantial role, especially in the provision of fast regulation services among AS, such as primary and secondary frequency control [5,6]. Electrical storage can accommodate large ramping rates, can both inject and absorb power to and from the grid, and does not exhibit dynamic inertia when power flow changes direction [7]. The limiting constraint for the mass adoption of storage systems for AS is their high acquisition cost and significant ageing at high c-rates.

A promising alternative is to utilize resilient battery systems that have a different primary purpose (e.g. storage supporting fast-charging stations) when they are standing idle. This necessitates that the primary function of the system will not be disturbed and that the control energy generated is compliant to regulations. Networks of systems are expected to be more suitable for this type of operation as a result of complementarities (allocation of service among them to mitigate control energy requests) and robustness (distributed systems are commonly more resilient to faults than an individual system) [8].

Electrification in transportation offers a potential candidate for this type of solution. Most ideas in the literature have been extensively examining the capacity of vehicle storage for provision of services to the grid [9,10], while fewer the potential that storage at charging stations can offer [11, 12]. We examine here the ABB TOSA electrical bus system in Geneva that employs fast-charging stations to limit the size of bus on-board batteries [13]. Between bus arrivals the storage system can offer control-energy to the grid while at the same time managing the state-of-charge to ensure that sufficient energy remains for a fast charge upon bus arrival. We design the control system in order to be able

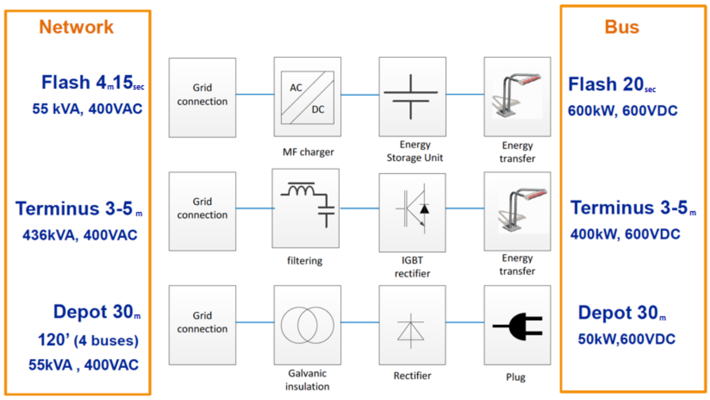

Figure 2: Main components of the ABB TOSA system infrastructure between the electrical network and the electrical bus.

to offer Secondary-Frequency-Control (SFC) according to the requirements of Swissgrid, the Transmission System Operator (TSO) of Switzerland. We use the hourly-price charges of the local utility company (Service Industriel de Genève - SIG) to calculate energy costs with and without provision of AS.

The results show that a considerable amount of control-energy can be generated by a network of storage systems without disturbing the primary function of the network which is fast-charging. An ageing study conducted with a proprietary tool of ABB indicates that AS provision has minor ageing effects for the resilient type of batteries employed in ABB TOSA charging stations. The flexibility generated can be sold to an aggregator or directly to the Swissgrid secondary market for AS for a considerable economic benefit.

Section 2 provides an overview of the ABB TOSA system, Section 3 describes the AS market in Switzerland, Section 4 details the control and method architecture used , Section 5 studies the economic effects of AS provision on the operation of ABB TOSA and Section 6 outlines the results of the ageing study on the battery systems, while Section 7 offers concluding remarks to the methodology and its benefits.

2 ABB TOSA System

ABB TOSA[1] is a fully electric, high-capacity, articulated bus that runs without overhead lines. The bus is equipped with a 40 kWh battery and a system for automatic energy transfer. When the bus pulls into a charging stop it connects to a high-power charging contact, as in Figure 1, and charges its batteries during the time its passengers are embarking and disembarking. A flash charge of 20 seconds at 600 kW is provided to allow the bus to continue its trip until the next charging point. Flash charging stations are a design choice that allows for smaller batteries on-board, optimizing equipment cost and minimizing the weight carried by the bus.

[1] Trolleybus Optimisation du Systme d'Alimentation

Figure 2 summarizes the main components of the charging infrastructure of ABB TOSA. Flash chargers are placed at selected spots along the route of the bus. Because high-power charging can result in load peaks affecting the local grid, the flash charger station flattens out demand by utilizing highly resilient batteries located on the wayside drawing a lower current from the grid. At the terminus of the line, where buses are scheduled to stop for longer periods, more prolonged charges of three to five minutes at 400 kW are delivered to the bus. This additional flash-charging stop was created to avoid increased operating costs for the bus service (to decrease long waiting times that affect schedule frequency and driver man-hours). A third type of charger is utilized for the bus-depot, where a longer charge is applied to compensate the energy required between the operating line and depot location. Since there is sufficient time for charging at the depot a flash-charging station is not required at this location.

For our analysis we use the configuration of TOSA for Line 23 of Geneva, that carries more than 10'000 passengers a day between the airport and the city. ABB has deployed 12 flash-charging stations along the 27 km (roundtrip) urban transit bus route, as well as three terminal and four depot feeding stations. The flash-charging stations are equipped with highly resilient LTO batteries with a 90 kWh storage capacity each. In order to satisfy fast-charging requirements their State-of-Charge (SoC) has to be at least 65% at bus arrival (otherwise more time is required for charging which may disrupt the bus schedule). A fleet of 12 electrical buses is utilized along the line that generate an average of 900 charging requests per day. Bus speeds are considered stochastic varying ±50% over nominal speed for arrival according to schedule.

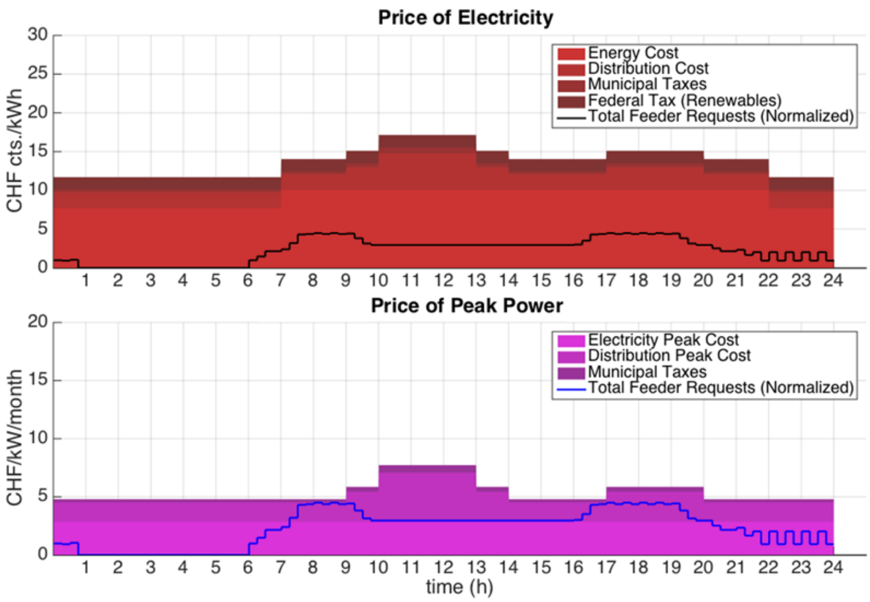

Figure 3: Price of energy (up) and peak power cost (down) at different hours of SIG for large customers. Aggregate bus feeder flash requests displayed for comparison.

Energy is procured directly from the EPEX spot market (day-ahead and intraday). The electricity distribution provider for TOSA is SIG (Service Industriels de Genève), the local utility company of Geneva. To accurately reflect the economic effect of AS provision in the operation of the system, we incorporate in our analysis the real tariffs of SIG in terms of distribution charges and peak-demand charges as well as taxes and municipal fees. SIG utilizes time-variable tariffs with peak and off-peak costs that mostly coincide with the peak usage of the line, as shown in Figure 3.

3 Ancillary Services

Grid operators need to balance demand and supply of electricity at all times to maintain stable operation. To achieve this the grid operator procures reserve power capacity, known as AS. Traditionally, these services have been provided by power generators, but recently a lot of research has been done to enable loads and storage devices to also provide AS. AS can be divided into three main categories based on their time scales - primary, secondary, and tertiary.

In this study we focus on the provision of secondary frequency control (SFC) service to the grid using batteries and particularly using a group of TOSA bus charging batteries. There are two phases of operation for loads to provide SFC service to the grid - offline, and online.

Notation: Bold letters denote sequence of vectors over time, the length of which is clear from context, e.g., $\mathbf{e} = [e_0^T, e_1^T, ..., e_{N-1}^T]^T$.

3.0.1 Offline Phase

During the offline phase of operation the load needs to declare the nominal (or baseline) consumption $\mathbf{P^{DA}}$ over a certain period of time (usually one day), and a flexibility γ around the baseline. Together these two quantities define the set of all the power trajectories ($\mathbf{P^{DA}} \pm \gamma$) that the grid can ask the load to follow during the online phase of operation.

3.0.2 Online Phase

During the online phase of operation the load can modify its day-ahead declared baseline, with a certain delay[2], by trading energy on the intraday market. The effective baseline is then the sum of the day-ahead baseline $\mathbf{P^{DA}}$ and the intraday modifications $\mathbf{P^{ID}}$.

The load receives a normalized regulation signal from the grid operator which indicates the desired increase or decrease in consumption relative to the baseline ($\mathbf{P^{DA}} + \mathbf{P^{ID}}$). The regulation signal is named differently in different countries, and is known as the Area Generation Control (AGC) signal in Switzerland. The magnitude of the required deviation from the baseline is determined by the flexibility γ which is fixed during the online phase. The load is required to track the received AGC signal within a certain allowed error range ϵ. This means that the load has to make sure that its total power consumption P_k is close enough to the sum of the baseline ($P_k^{DA} + P_k^{ID}$) and the scaled version of the received

[2]The intraday market delay is 30 minutes according to current Swiss regulations.

AGC signal (γa_k), which is expressed as

$$\|P_k - P_k^{DA} - P_k^{ID} - \gamma a_k\|_\infty \leq \epsilon \quad (1)$$

where ϵ is the allowed tracking error.

4 Control Systems for AS Provision

This section presents the mathematical model of the electric batteries, and the controller for the offline and online phase of operation that enables the network of bus charging batteries to provide SFC to the grid.

4.1 Electric Batteries

The TOSA electric batteries are installed at the passenger stations to flash charge the buses while the passengers get on and off of the bus. The mathematical model of a TOSA battery is given as

$$s_{k+1} = s_k + \eta_g u_k^b - \eta_f u_k^f \quad (2)$$

where s_k is the state-of-charge (SOC), u_k^b is the electrical power consumption from the grid, and u_k^f is the power for flash charging the bus at time step k. The efficiency for charging the battery from the grid and flash dis-charging to the bus is denoted by η_g and η_f, respectively. The SOC and the charge / discharge powers are required to be within the operational constraints of the battery which are expressed as

$$s_{\min} \leq s_k \leq s_{\max} \quad (3)$$

$$u_{\min} \leq u_k^b \leq u_{\max} \quad (4)$$

The SOC of the battery is required to be above a certain limit s^f to enable flash dis-charging, therefore, it is constrained to be above s^f at the times of bus arrival

$$s_k \geq s^f, \qquad \forall k \in \mathcal{K}_f \quad (5)$$

where $\mathcal{K}_f$ is the set of time steps corresponding to the bus arrival times. Moreover, the battery is not allowed to charge from the grid when it is flash charging the buses, resulting in

$$u_k^b = 0, \qquad \forall k \in \mathcal{K}_f \quad (6)$$

4.1.1 Network of Batteries

The states and inputs of the individual battery models can be stacked to formulate the centralized state-space model of all the electric batteries in the network. The stacked states and inputs are defined as, $S_k = [s_k^1, s_k^2, \ldots, s_k^n]^T$, $U_k^b = [u_k^{b,1}, u_k^{b,2}, \ldots, u_k^{b,n}]^T$, and $U_k^f = [u_k^{f,1}, u_k^{f,2}, \ldots, u_k^{f,n}]^T$, where s_k^i, $u_k^{b,i}$ and $u_k^{f,i}$ are the state and inputs of the i^{th} battery, and n is the total number of batteries in the network.

The centralized state-space model is used to define the set of feasible power inputs to the network of batteries, and is given as

$$\mathcal{U}^b(S_0, \mathbf{U}^f) = \left\{ \mathbf{U^b} \;\middle|\; \begin{array}{l} S_{k+1} = S_k + H_g U_k^b - H_f U_k^f \\ s_{\min} \le S_k \le s_{\max} \\ u_{\min} \le U_k^b \le u_{\max} \\ \forall k = 0, \ldots, N-1 \\ s_k^i \ge s^f, \qquad \forall k \in \mathcal{K}_f^i \\ u_k^{b,i} = 0, \qquad \forall k \in \mathcal{K}_f^i \\ \forall i = 1, \ldots, n \end{array} \right\} \tag{7}$$

where H_g and H_f are diagonal matrices of appropriate sizes, containing the efficiencies of individual batteries, and $\mathcal{K}_f^i$ is the set of time steps corresponding to the bus arrival times at the i^{th} battery. The set (7) defines all the trajectories of power consumption over a horizon of N, that the network of batteries can consume, while staying within operational constraints. Note that this set is a function of the initial state S_0 and the flash dis-charging power $\mathbf{U}^f$ of the batteries.

4.2 Offline Phase

This section presents the controller for the offline phase of operation which is at the beginning of the activation period. During this phase, the network of batteries are required to fix a day-ahead baseline $\mathbf{P^{DA}}$ over a certain horizon (typically one day) and a flexibility γ around the baseline that is committed to the grid. This phase is repeated after a horizon of N (which is typically one day).

4.2.1 Economic Optimization

The optimization problem for the offline phase of operation is formulated as

$$\begin{aligned} &\underset{\gamma, \mathbf{P^{DA}}, \pi_b, \pi_{ID}}{\text{minimize}} \quad \mathbb{E}_{\mathbf{a}} \left\{ J(\gamma, \mathbf{P^{DA}}, \mathbf{P^{ID}}, \mathbf{a}) \right\} \\ &\text{s.t.} \\ &\text{(Battery feasibility)} \quad \mathbf{U^b} \in \mathcal{U}^b(S_0, \mathbf{U^f}) && (8) \\ &\text{(Total power)} \quad \mathbf{P} = \Gamma \mathbf{U}^b && (9) \\ &\text{(Power tracking)} \quad \|\mathbf{P} - \mathbf{P^{DA}} - \mathbf{P^{ID}} - \gamma \mathbf{a}\|_\infty \le \epsilon && (10) \\ &\text{(Power flexibility)} \quad \gamma \ge 0 && (11) \\ &\text{(Move-blocking)} \quad T\mathbf{P^{DA}} = \mathbf{0}, \quad T\mathbf{P^{ID}} = \mathbf{0} && (12) \\ &\text{(Control Policies)} \quad \mathbf{U}^b = \pi_b(\mathbf{a}), \quad \mathbf{P^{ID}} = \pi_{ID}(\mathbf{a}) && (13) \\ &\text{(Uncertainty set)} \quad \forall \mathbf{a} \in \Xi && (14) \end{aligned}$$

where J is the economic cost of operation and is typically a function of the day-ahead baseline, flexibility, and the intra-day trades. The exact formulation and components of the cost function can vary according to the regulations in different markets (countries), and more details are given in Section 5.

The operational constraints of the network of batteries are represented by (8), while the total power consumption of all the batteries over the horizon is denoted by $\mathbf{P}$ and is given by (9), where $\Gamma := I_N \otimes \mathbf{1^T}$, with I_N an identity matrix of size N, and $\otimes$ is the Kronecker product. The requirements of tracking the AGC signal is expressed in (10), and the flexibility γ is constrained to be positive in (11). Equation (12) is a move-blocking constraint (see e.g., [14]) which ensures that the day-ahead baseline and the intra-day modification in the baseline are fixed for a certain number of time-steps, using an appropriate move-blocking matrix T. This is because the AS market regulations typically allow $\mathbf{P^{DA}}$ and $\mathbf{P^{ID}}$ to vary at a slower rate than the rest of the variables in the optimization problem.

The AGC signal $\mathbf{a}$ is uncertain and unknown at the time of solving this problem and is assumed to lie in the uncertainty set Ξ (14) (the set Ξ is defined in more detail below in (18)), therefore an expectation is taken over $\mathbf{a}$ in the cost function. The uncertainty is revealed progressively during the online phase, and it is possible to change the power input to the batteries $\mathbf{U}^b$ and the intra-day control action $\mathbf{P^{ID}}$ as the uncerainty is revealed during the online phase, therefore, $\mathbf{U}^b$ and $\mathbf{P^{ID}}$ are not optimization variables, and are defined by causal control policies π_b, and π_{ID} in (13).

The optimization problem for the offline phase is a multi-stage stochastic problem of combinatorial complexity. An approximate solution method, similar to the one developed in [15] is used to solve the problem. The key idea of the method is to optimize the intraday policy separately, and to approximate the rest of the problem by a two-stage robust problem with intraday policy already fixed.

4.2.2 Intraday control

During the online phase, intraday trades can be used to modify the day-ahead declared baseline with a certain delay which is a useful feature for energy constrained loads, e.g., batteries providing AS because the intraday market can be used to remove the bias in the AGC signal, resulting in a higher offered flexibility to the grid. This is because a given physical resource (storage device) can provide a higher flexibility when it is asked to track an AGC signal with lower energy-content, or which is close to zero-mean. The intraday policy used in this paper is taken from [15], and is described briefly for the clarity of the manuscript.

We define the residual tracking signal as the effective regulation signal with respect to the day-ahead baseline after making the intraday adjustments, and it is the sum of the AGC signal and the normalized intraday control action

$$\mathbf{r} = \mathbf{a} + \mathbf{\bar{P}^{IN}} \tag{15}$$

where $\mathbf{\bar{P}^{IN}}$ is the normalized intraday control action, i.e., $\mathbf{P^{IN}} = \gamma\mathbf{\bar{P}^{IN}}$. The tracking constraint in (10) can be reformulated in terms of the residual tracking signal as

$$\|\mathbf{P} - \mathbf{P^{DA}} - \gamma\mathbf{r}\|_\infty \le \epsilon \tag{16}$$

The intraday policy is defined as

$$\pi_{ID}(\mathbf{a}) := \left\{\mathbf{\bar{P}^{ID}} \,\middle|\, \bar{P}^{ID}_{k+1} = f(a_k, \bar{P}^{ID}_k, \mathbf{\tilde{a}})\right\} \tag{17}$$

The goal of the intraday policy is to minimize the energy content (cumulative sum) of the residual tracking signal by making appropriate intraday transactions at each time step, while also respecting the market delay. It is a causal policy, and determines the future intraday trades at each time step, as a function of the past AGC signal, past intraday control actions, and historic AGC scenarios $\tilde{\mathbf{a}}$. The reason behind this approach is to separate the intraday control policy from the bidding problem and to solve it independently. The bidding problem can be approximated by a two stage stochastic optimization problem using the pre-defined intraday policy. More details of this method can be found in [15].

Note that the intraday control policy (17) can be used to compute a trajectory of residual tracking signal corresponding to a given trajectory of the AGC signal. Note also that the policy (17) is designed to incorporate the move-blocking constraint (12) to make sure that the intraday actions are at the appropriate time-step.

4.2.3 Uncertainty set

The uncertainty set Ξ is constructed as a convex hull of a finite number N_s of historic AGC signals and is given as

$$\Xi = \left\{ \sum_{j=1}^{N_s} \lambda^j \tilde{\mathbf{a}}^j \mid \sum_j \lambda^j = 1, \lambda^j \geq 0 \right\} \tag{18}$$

where $\tilde{\mathbf{a}}$ is the previously observed AGC signal scenarios.

4.2.4 Flash charging and bus arrival

The bus arrival schedule at each charging station is fixed and is known in advance. This data is used to construct the sets $\mathcal{K}_f^i$ needed to solve the problem. Moreover, flash charging power requested by the buses at the charging stations is also constant and known in advance, and can be used together with the arrival schedules to formulate the trajectory of flash charging power $\mathbf{U^f}$ over the horizon which is needed to solve the optimization problem.

4.2.5 Approximate solution

The economic optimization problem presented in Section 4.2.1 is approximated by a tractable two-stage robust optimization problem using the intraday control policy (17) and the uncertainty set Ξ (18). The multi-stage structure of the original problem is reduced to two stages where the day-ahead baseline $\mathbf{P^{DA}}$ and the flexibility γ are the first stage decision variables, while the total power $\mathbf{P}$ and the power consumption of the batteries $\mathbf{U^b}$ are second-stage variables.

The resulting tractable problem is given as

$$\underset{\gamma,\mathbf{P^{DA}}}{\text{minimize}} \quad \frac{1}{N_s}\sum_{j=1}^{N_s} J(\gamma, \mathbf{P^{DA}}, \mathbf{P^{ID,j}}, \mathbf{r^j})$$

$$\text{s.t.}$$

$$\begin{aligned}
&\text{(Battery feasibility)} \quad \mathbf{U}^{b,j} \in \mathcal{U}(S_0, \mathbf{U}^f) && (19)\\
&\text{(Total power)} \quad \mathbf{P}^j = \Gamma \mathbf{U}^{b,j} && (20)\\
&\text{(Power tracking)} \quad \|\mathbf{P}^j - \mathbf{P^{DA}} - \gamma \mathbf{r}^j\|_\infty \leq \epsilon && (21)\\
&\text{(Power flexibility)} \quad \gamma \geq 0 && (22)\\
&\text{(Move-blocking)} \quad T\mathbf{P^{DA,j}} = \mathbf{0} && (23)\\
&\forall j = 1, \ldots, N_s && (24)
\end{aligned}$$

where N_s is the number of scenarios of the uncertain parameter, and the superscript j denotes the separate trajectory of the second stage decision variables corresponding to each trajectory of the uncertain parameter (residual tracking signal), implicitly defining the control policy. The intraday policy is already fixed by (17), and is used to generate scenarios of the residual tracking signal $\mathbf{r}$ corresponding to each scenario of the AGC signal in set Ξ. The expectation in the cost function is approximated empirically using scenarios of the residual tracking signal.

The solution of the approximate problem results in the optimal day-ahead baseline $\mathbf{P^{DA*}}$ and flexibility γ^* which are used during the online phase.

4.3 Online Phase

The objective of the online phase of the ancillary service provision is to track the total power reference provided to the TOSA system while preserving system safety. This objective can be achieved with a two-layer control structure as shown in Figure 4. The upper layer operates at a slow time-scale and decides on the realizations of the intraday trades $\mathbf{P^{DA}}$ while the lower layer directly controls the charging inputs for the TOSA batteries.

4.3.1 Intraday controller

Online intraday trades are decided by an MPC layer that takes into account the measured SoC of the batteries and the prediction of the AGC signal. The MPC problem is solved every hour, 30 minutes before the realization of the intraday trade for a time-slot, as required by the market regulation. The main objective of the intraday controller is to ensure AGC tracking constraint (16) is satisfied. Additional objectives can be added, reflecting the economics or the safety of the battery system. We choose a cost function that targets a medium level total SoC reference away from the limits for the whole fleet of batteries at the end of the intraday period.

The control problem is formulated as a two-stage stochastic problem, similar to the bidding problem. The first stage decision is the intraday trade realization for the next hourly slot, while the second stage decision is the charging of the TOSA batteries, given the intraday trade decision, the expected bus arrival times and the AGC reference. Since the AGC reference is not known ahead

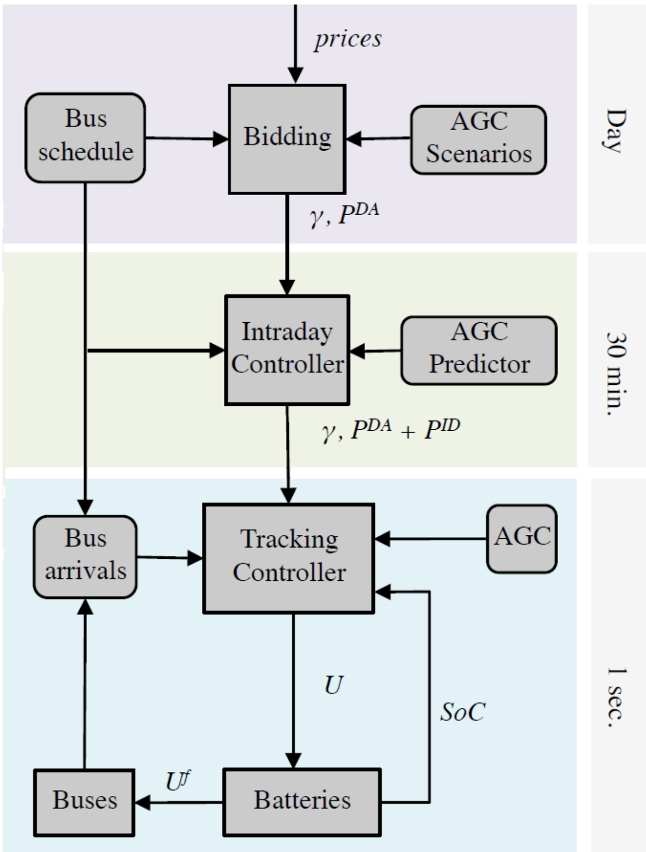

Figure 4: Block diagram of the control architecture.

of time, we use a statistical predictor to generate scenarios. The prediction horizon is limited to 90 minutes, which covers the effective one hour period of the next intraday trade at the time the problem is solved, with a sampling rate of 1-minute. The resulting intraday control problem can be formulated as

$$\begin{aligned}
\underset{\mathbf{P^{ID}}}{\text{minimize}} \quad & \frac{1}{N_s}\sum_{j=1}^{N_s}\left(\sum_{i=1}^{n} S_{90} - n\mathbf{S}_{\text{ref}}\right) \\
\text{s.t.} \quad & \\
\text{(Battery feasibility)} \quad & \mathbf{U}^{b,j} \in \mathcal{U}(S_t, \mathbf{U}^f) && (25)\\
\text{(Total power)} \quad & \mathbf{P}^j = \Gamma \mathbf{U}^{b,j} && (26)\\
\text{(Power tracking)} \quad & \|\mathbf{P}^j - \mathbf{P^{DA}} - \mathbf{P^{ID}} - \gamma \mathbf{r}^j\|_\infty \leq \epsilon && (27)\\
\text{(Piecewise constant)} \quad & T^{ID}\mathbf{P^{ID}} = \mathbf{0} && (28)\\
\text{(Previous trade)} \quad & P^{ID}_k = P^{ID}_{-1},\ k = 1, \ldots, 30 && (29)\\
& \forall j = 1, \ldots, N_s && (30)
\end{aligned}$$

The reference SoC value $\mathbf{S}_{\text{ref}}$ is chosen as the mean of the minimum and max-

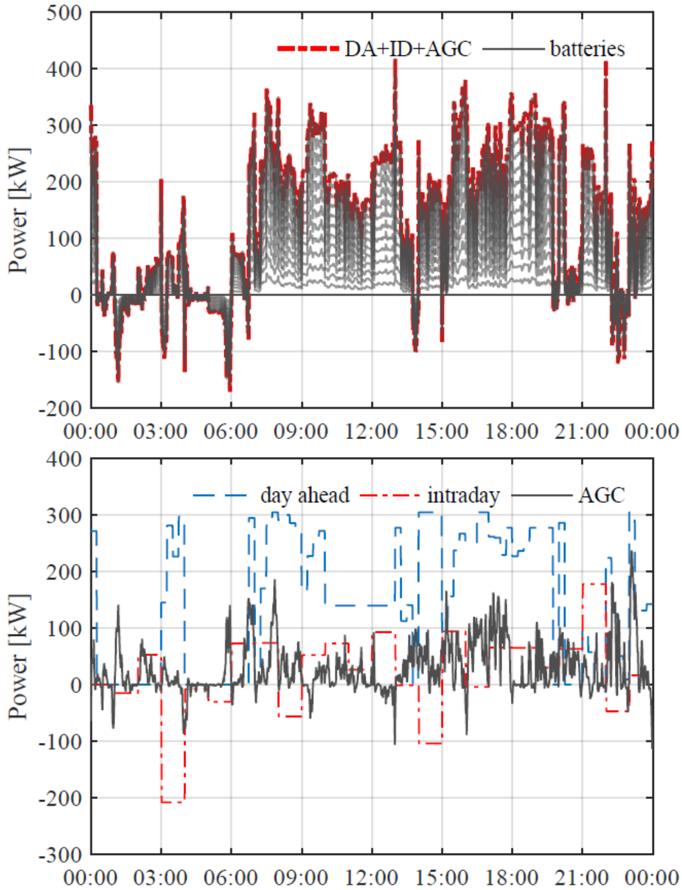

Figure 5: Top: Allocation of total power charging reference among the 12 TOSA batteries for a daily operation. Bottom: Realizations of the day-ahead, intraday and the AGC signal for the same day.

imum bounds for the SoC, $s_{\min}$ and $s_{\max}$ whereas S_{90} indicates the SoC level at the end of the horizon of 90 minutes. The first 30 minutes of the prediction horizon is covered by the previous trade agreement with value P_{-1}^{ID}, which is enforced by constraint (29).

4.3.2 Tracking controller

The tracking controller resides at the lowest layer of the control structure and directly interacts with the batteries. The controller operates at a fast rate of 1 second and determines the charging/discharging levels for the batteries.

The available information to the controller in real-time is the current values of the reference for the total power injection to the grid, flash charging of buses and the SoC of the batteries. We use a simple control logic that allocates the total power reference amongst batteries in a way that prioritizes the batteries

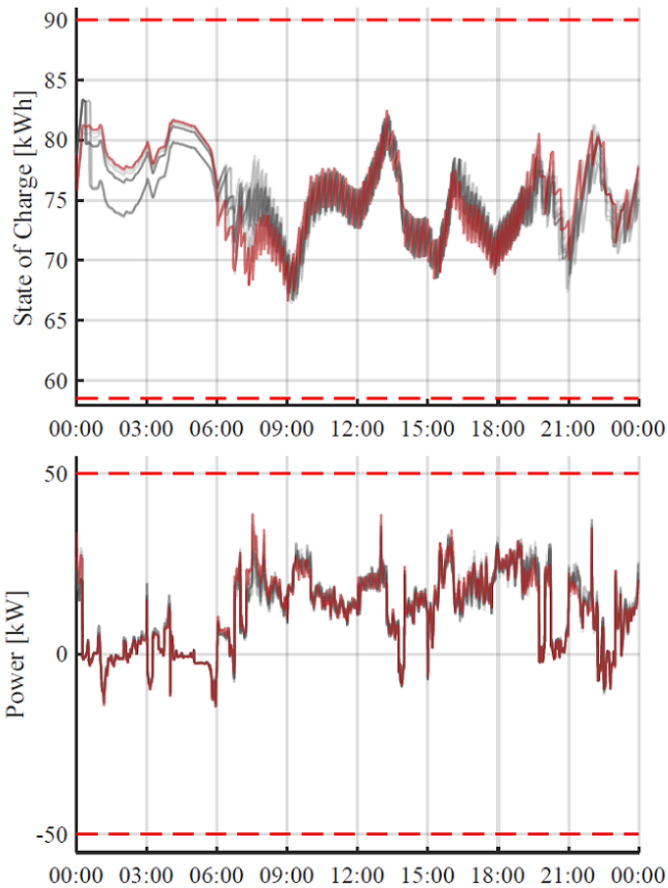

Figure 6: State of charge and charging power trajectories for the 12 TOSA batteries during daily operation. The trajectories of battery 1 are highlighted.

with larger available SoC margins. For battery i, the margins are computed as

$$\begin{aligned} \Delta S^i_- &= \max(S^i_{\text{ref}} - s_{\min}, 0) \\ \Delta S^i_+ &= s_{\max} - S^i_{\text{ref}} + \Delta t P^i_f \end{aligned} \tag{31}$$

where Δt is the sampling time. Note that flash charging increases the upward state of charge margin, since it will have a decreasing effect on SoC. The downward margin is saturated when it becomes negative as it is possible for the battery to have a SoC level below $s_{\min}$ immediately after a flash charging action. The allocation of the power reference to each battery is computed as

$$\begin{aligned} P \leq 0 &\Rightarrow P^i = P \frac{\Delta S^i_-}{\sum_{i=1}^n \Delta S^i_-} \\ P > 0 &\Rightarrow P^i = P \frac{\Delta S^i_+}{\sum_{i=1}^n \Delta S^i_+} \end{aligned} \tag{32}$$

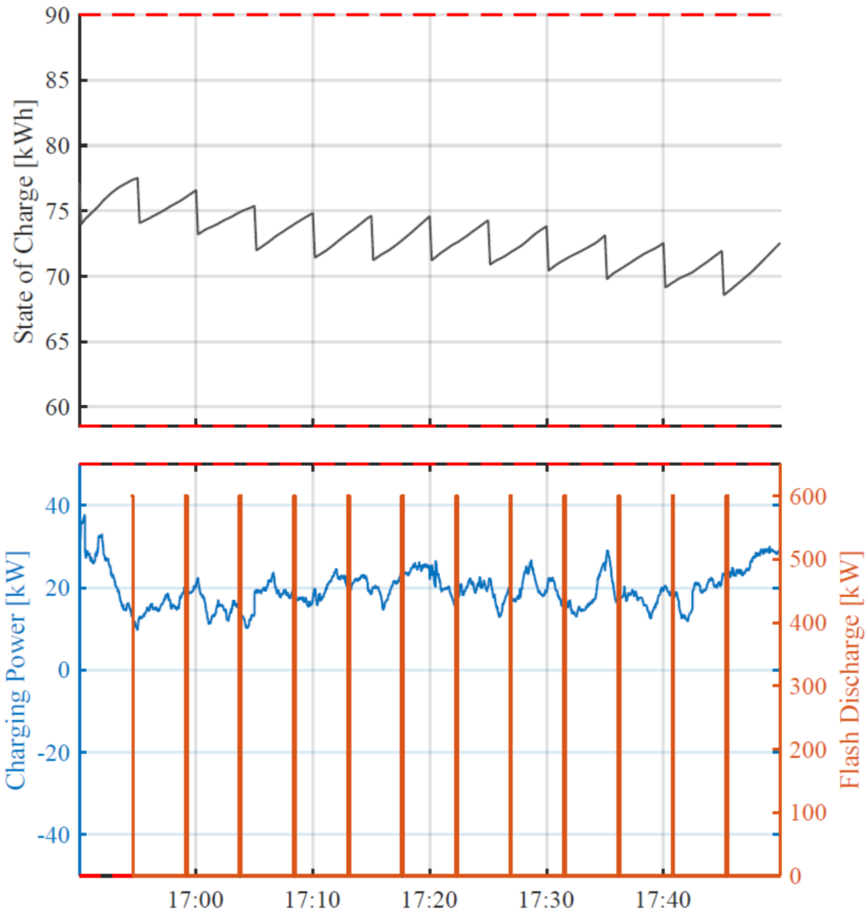

Figure 7: Detailed view of the SoC, charging and discharging power trajectories for battery 1.

4.4 Validation of the Control Scheme

The proposed control approach together with the stochastic programming based flexibility bidding scheme is validated with randomly sampled AGC signals and bus arrival times. The results for an example day are shown in Figures 5, 6 and 7. The hierarchical control scheme is able to preserve the feasibility of the batteries in terms of SoC and charging limits, while being able to provide precise tracking of the AGC signal.

5 Economic Analysis

This section discusses the economic aspects of using the TOSA batteries for the provision of SFC service.

5.1 Cost components

The systemy providing SFC service to the grid are required to interact with different energy markets, and their total operational cost is a sum of several different components. These components of the total cost are briefly described below.

5.1.1 Baseline cost

the cost of buying baseline energy $\mathbf{P^{DA}}$ in the day-ahead energy market. The price of this energy is time-varying and here is the sum of the spot market price with distribution charges, and taxes from the local utility company.

5.1.2 Capacity revenue

the revenue received for providing reserve flexibility (SFC service) in the AS market, despite of whether is is activated.

5.1.3 Tracking penalty

the penalty one has to pay if not able to track the AGC signal, proportional to the tracking error.

5.1.4 Tracking bonus

Tracking the AGC signal is incentivized by paying a lower price (or receiving a rebate) for the extra (or the lower) electricity consumed compared to baseline, while tracking a consumption AGC signal.

5.1.5 Intraday cost

It is the cost (or income) of buying (or selling) energy $\mathbf{P^{ID}}$ in the intraday market for making the required adjustments in the dayahead baseline. The price of this energy is usually close to the price of day-ahead baseline.

5.1.6 Peak cost

the cost for the peak consumption during a certain period of time. These costs are imposed to avoid overloading the distribution grid.

5.1.7 Total cost

The total energy-related cost of operation is the sum of the six components described above.

5.2 Economic comparison

We carried out a simulation based financial analysis to evaluate the economic potential of providing SFC service using the TOSA batteries. The base case for comparison is the default operation of the TOSA batteries when only serving their primary purpose of bus charging, without providing the SFC service. A control scheme similar to the one in Section 4 is used with the objective of

Charging Station Battery		
Storage capacity (s_{max})	90	kWh
Maximum power (u_{max})	50	kW
Flash power (u^f)	600	kW
Min. SOC at flash (s^f)	58.5	kWh
Number of stations	12	

Table 1: TOSA charging station battery parameters

minimizing the total cost of default operation.For the SFC provision case, the control scheme presented in Section 4 is used with the objective of minimizing the total cost of operation.

5.2.1 Simulation setup

Simulations are carried out using the real AGC data received from Swissgrid for the year 2014. The price data for all the cost components described in Section 5.1 are obtained from EPEX, SIG and Swissgrid. Daily average prices of all the cost components are used in simulations. During the offline phase, the economic optimization problem is solved at the beginning of the day with an horizon of one day. The day-ahead baseline and intraday modifications are sampled at 15 minutes (using the move-blocking constraint). During the online phase, the intraday controller runs every minute, while the the tracking controller runs every second to track the received AGC signal. Specifications of the TOSA batteries used in the simulations are given in Table 1.

5.2.2 Results

The average monthly energy related costs of operation for both cases - default and SFC provision are reported in Table 2. The results show that on average, the energy-related cost of operating the TOSA batteries is decreased by about 37% by providing the SFC service. A closer look at the individual cost components reveals that when providing SFC service, the cost of baseline is increased. This is for the extra energy needed to achieve flexibility in both directions. The tracking bonus is very small because it is mostly cancelled out between negative and positive AGC commands. The tracking errors are always within the allowed range, and are very small in terms of costs. The intraday cost is also small because on average, the negative and positive trades almost cancel out each other. Peak costs are increased significantly because the peak consumption of the batteries increases when tracking a large AGC command. However, the increase in the baseline and the peak costs is compensated by the revenue received by providing flexibility, resulting in a significant reduction in the overall operational cost compared to the default case.

6 Battery Ageing Analysis

In order to estimate the effect of the provision of AS to the lifetime of the TOSA batteries an ageing analysis was conducted using “Battery ToolBox” (BTB), a proprietary ABB simulation tool. BTB is using both first-principles

	Default operation (CHF.)	SFC Provision (CHF.)
Baseline cost	9'102	10'018
Capacity Revenue	0	6'178
Tracking Bonus	0	199
Tracking Penalty	0	36.4
Intraday cost	0	230
Peak cost	1'474	2'790
Total cost	10'576	6'698

Table 2: Total monthly cost of operation and cost components - Comparison between default operation of the TOSA batteries and the SFC provision case.

models and experimental data to perform the analysis, includes a library of real battery models, relevant inverter models, and can conduct electrical, thermal and ageing simulations. The ageing analysis in BTB considers the interplay of several mechanisms such as calendar ageing, cycling, temperature, SoC, DoD and C-rate which are considered relevant and sufficient for the comparisons presented here.

To assess the ageing effects of AS provision, we used BTB to run simulations of TOSA batteries under default operation and under AS provision mode for a period of 240 hours. The results for the effects of the two operational modes on the State of Health (SoH) are shown in Figure 8. The SoH for default mode is 97.43%, while for AS provision it is 97.36%. This shows an almost negligent difference in ageing. This result is corroborated by the average c-rate imposed by the two modes which is 0.249 and 0.258, respectively.

The very small difference in ageing between the two modes is due to the TOSA batteries having been designed for very high c-rates (600 kW each) to enable flash-charging. Available flexibility for AS provision, computed with the method presented here, is usually 200-250 kW in total which means at most 20 kW of per battery. Moreover, this reserved flexibility is rarely activated at its maximum but mostly below 50%.

This important outcome indicates that the battery assets of the TOSA system can be utilized for AS provision, without a significant impact on their lifetime.

7 Conclusion

We have demonstrated here, how the EV-charging infrastructure of an electrical bus system can be effectively used for the provision of AS to the power grid. The flexibility of the system can be quite significant (250 kW of flexibility for 900 kWh of storage) despite the requirements of its primary purpose (flash charging incoming buses) and despite limiting the size of the system to one line. The system can be easily scaled to a larger number of bus lines, in the same city and in multiple locations across the transmission system. This could lead to a significant increase of the total flexibility offered and potential synergies between the multiple integrated systems.

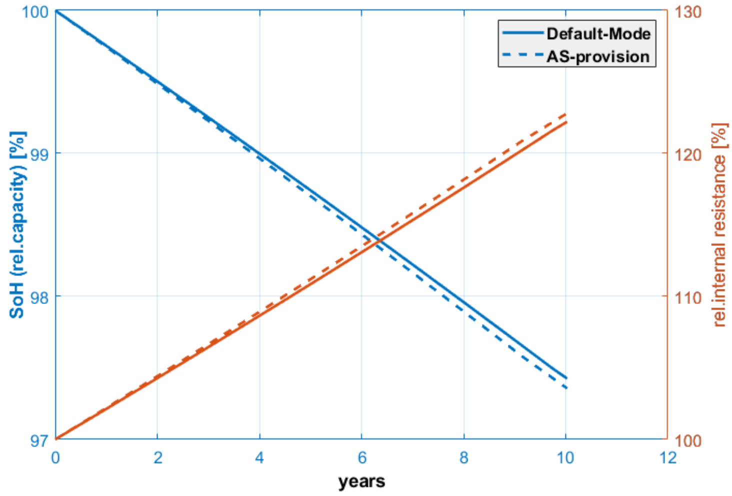

Figure 8: State of Health of the batteries according to mode of operation (default and AS - SFC provision).

The provision of AS has also significant economic benefits, even for the strict requirement of the Swiss TSO. A change in the economic parameters could have an additional impact, especially concerning peak power charges, since AS are offered through the distribution network. An even larger potential can be expected for provision of time-varying flexibility, either due to a relaxed regulation framework, or to a VPP that can combine this service with other assets. Finally, the very low effect in the ageing of the batteries indicates that AS provision for EV-charging infrastructure is a service that can be integrated without impacting the system lifetime.

Acknowledgment

This project has received funding from the European Research Council (ERC) under the European Unions Horizon 2020 research and innovation programme (grant agreement No 755445). We would like to thank Swissgrid Ltd. for providing us with all the relevant data for our simulation studies.

References

[1] I. Secretariat, "Global EV Outlook 2017," International Energy Agency, Tech. Rep., 2017.

[2] B. E. economics, "BP Energy Outlook 2018," BP energy economics, Tech. Rep., 2018.

[3] M. Liserre, T. Sauter, and J. Y. Hung, "Future energy systems: Integrating renewable energy sources into the smart power grid through industrial electronics," *IEEE industrial electronics magazine*, vol. 4, no. 1, pp. 18–37, 2010.

[4] F. Mwasilu, J. J. Justo, E.-K. Kim, T. D. Do, and J.-W. Jung, "Electric vehicles and smart grid interaction: A review on vehicle to grid and renewable energy sources integration," *Renewable and Sustainable Energy Reviews*, vol. 34, pp. 501–516, 2014.

[5] K. Divya and J. Østergaard, "Battery energy storage technology for power systemsan overview," *Electric Power Systems Research*, vol. 79, no. 4, pp. 511–520, 2009.

[6] E. Sortomme and M. A. El-Sharkawi, "Optimal scheduling of vehicle-to-grid energy and ancillary services," *IEEE Transactions on Smart Grid*, vol. 3, no. 1, pp. 351–359, 2012.

[7] P. Mercier, R. Cherkaoui, and A. Oudalov, "Optimizing a battery energy storage system for frequency control application in an isolated power system," *IEEE Transactions on Power Systems*, vol. 24, no. 3, pp. 1469–1477, 2009.

[8] D. Pudjianto, C. Ramsay, and G. Strbac, "Virtual power plant and system integration of distributed energy resources," *IET Renewable Power Generation*, vol. 1, no. 1, pp. 10–16, 2007.

[9] S. B. Peterson, J. Whitacre, and J. Apt, "The economics of using plug-in hybrid electric vehicle battery packs for grid storage," *Journal of Power Sources*, vol. 195, no. 8, pp. 2377–2384, 2010.

[10] K. M. Tan, V. K. Ramachandaramurthy, and J. Y. Yong, "Integration of electric vehicles in smart grid: A review on vehicle to grid technologies and optimization techniques," *Renewable and Sustainable Energy Reviews*, vol. 53, pp. 720–732, 2016.

[11] Z. Wang and P. Liu, "Analysis on storage power of electric vehicle charging station," in *Power and Energy Engineering Conference (APPEEC), 2010 Asia-Pacific*. IEEE, 2010, pp. 1–4.

[12] S. Barsali, R. Giglioli, G. Lutzemberger, and D. Poli, "Optimal storage operation in ev charging stations delivering grid services," in *Environment and Electrical Engineering (EEEIC), 2016 IEEE 16th International Conference on*. IEEE, 2016, pp. 1–6.

[13] O. Augé, "Keynote 2: Tosa concept: A full electric large capacity urban bus system," in *Power Electronics and Applications (EPE'15 ECCE-Europe), 2015 17th European Conference on.* IEEE, 2015, pp. 1–1.

[14] R. Cagienard, P. Grieder, E. C. Kerrigan, and M. Morari, "Move blocking strategies in receding horizon control," in *2004 43rd IEEE Conference on Decision and Control (CDC) (IEEE Cat. No.04CH37601)*, vol. 2, Dec 2004, pp. 2023–2028 Vol.2.

[15] F. A. Qureshi, I. Lymperopoulos, A. A. Khatir, and C. N. Jones, "Economic advantages of office buildings providing ancillary services with intraday participation," *IEEE Transactions on Smart Grid*, vol. PP, no. 99, pp. 1–1, 2016.